nature portfolio

https://doi.org/10.1038/s41586-026-10322-z

Supplementary information

Gene regulatory landscape dissected by single-cell four-omics sequencing

In the format provided by the authors and unedited

Supplementary Table 1 | Summary of per-cell reagent costs for CHARM

Cost of enzymes and antibodies	
Enzymes and antibodies for bulk procedures	
Item	Cost per experiment ($)
Primary antibody	10
Secondary antibody	0.3
Tn5 transposase	12.8
pG-Tn5 transposase	12.8
Reverse Transcriptase	10
MboI	15
NlaIII	6
T4 DNA ligase	3.5
0.0352/cell (Based on 2,000 single cells isolated per bulk experiment)	
Enzymes for single-cell preamplification & library preparation	
Item	Cost per cell ($)
Deep Vent (exo-)	0.8
Tn5 transposase	1
KAPA HiFi DNA polymerase	0.5
	2.3/cell
Cost of other reagents and consumables	~ 1/cell
Total	~ 3.34/cell

Supplementary Table 2 | Identifier sequences for library type identification.

No.	Read type	Identification sequence
1	RNA	GGTTGAGGTAGTATTGCGCAATG
2	Histone modification	GGTTGAGGTAGTGGTATAGCTTCGTGTATAAGAGACAG
3	Accessibility	GGTTGAGGTAGTAAGTCCTGGATGTGTATAAGAGACAG

Supplementary Table 3 | Cell-cycle phase assignment criteria

Step	Cell-cycle phase	Assignment criteria
1	M	mean(mitotic%) > 0.2 or mean(farAvg) < 2.0e7
2	G2	mean(repli-score) < 0.5 & mean(near%) > 0.65
3	G1	mean(repli-score) < 0.5 & mean(G1S-score) > -0.2 & mean(G2M-score) < 0.1 & mean(near%) < 0.55
4	Early-S	mean(repli-score) < 0.57 & mean(G1S-score) > -0.2 & mean(G2M-score) < 0.1 & mean(near%) < 0.66
5	Late-S	mean(repli-score) < 0.57 & mean(G2M-score) > 0 & mean(near%) > 0.65
6	Mid-S	mean(repli-score) ≥ 0.55
7	Unknown	Remaining unassigned clusters

Supplementary Table 4 | Single-cell ordering criteria

No.	Cell-cycle phase	Sort order
1	Early-S	repli-score / var(repli-score) − mitotic% / var(mitotic%)
2	Mid-S	near% / var(near%)
3	Late-S	near% / var(near%) - repli-score / var(repli-score)
4	G1	near%
5	M and G2	maxbinorder

Supplementary Table 5 | Public ChIP-seq datasets used in this study

No.	Experiment target	File accession
1	BRD2	GSM4984767_ctr_rep_spikeIn_Brd2
2	BRD3	GSM4984768_ctr_rep_spikeIn_Brd3
3	BRD4	GSM4984769_ctr_rep_spikeIn_Brd4
4	CHD2	ENCFF927JDA
5	CTCF	ENCFF533APC
6	EP300	ENCFF460EOA
7	EZH2	GSE94300E14Ezh2
8	H3K27ac	ENCFF274UIB
9	H3K27me3	ENCFF008XKX
10	H3K36me3	ENCFF872CBV
11	H3K4me1	ENCFF426IIV
12	H3K4me3	ENCFF974BMC
13	H3K9ac	ENCFF514APY
14	H3K9me3	ENCFF348IAW
15	HCFC1	ENCFF058DYG
16	MAFK	ENCFF496JHC
17	MED1	SRR7262948Med1
18	NANOG	ENCFF097ISB
19	POLR2A	ENCFF128LHX
20	POU5F1	ENCFF058FSZ
21	PolII	SRR7262956PolIIr2
22	RAD21	GSM4984770_ctr_rep_spikeIn_Rad21
23	RING1B	GSE96107
24	SOX2	GSM3123485
25	ZC3H11A	ENCFF404QDD
26	ZNF384	ENCFF361ESB

Supplementary Table 6 | Validated enhancer-promoter pairs in mESC

Supplementary Table 7 | Cell-type-specific enhancer-promoter linkages predicted in the mouse brain

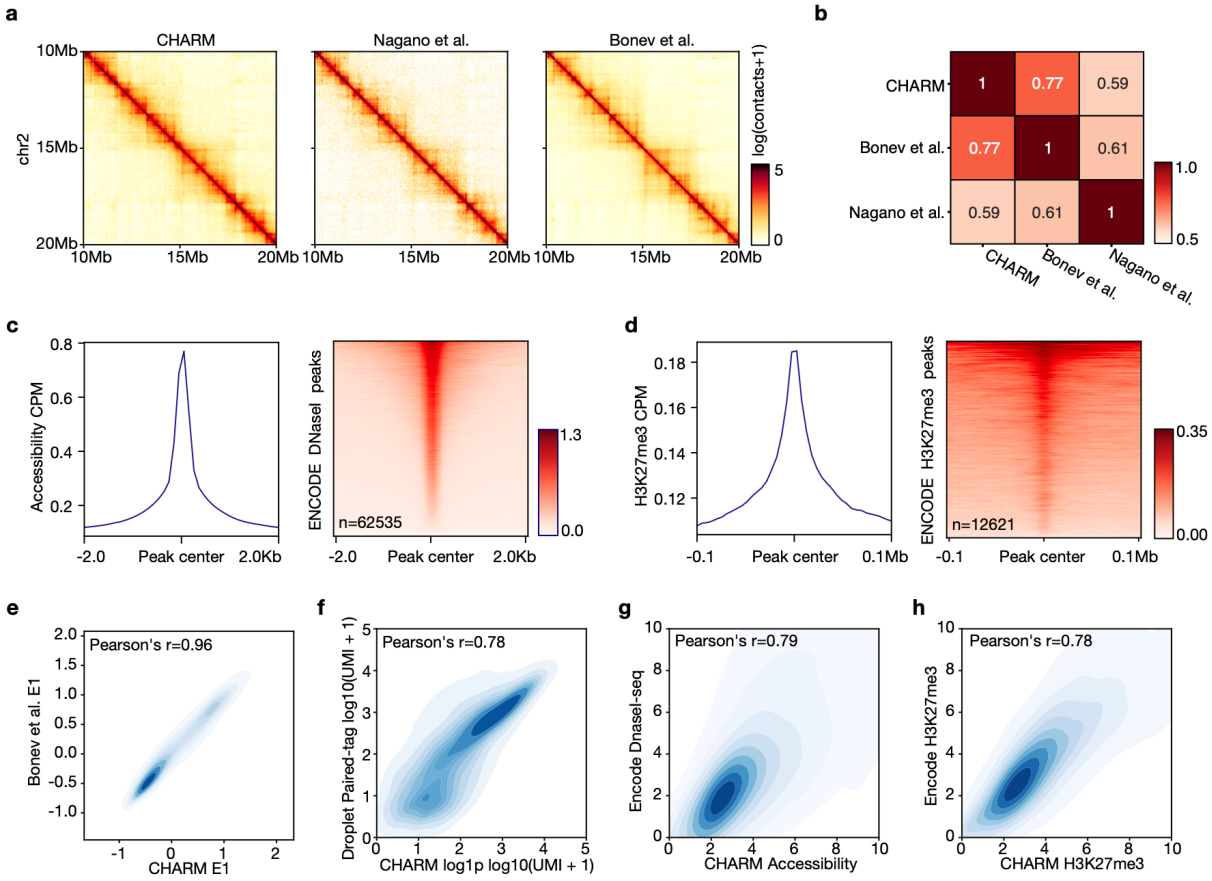

Supplementary Fig. 1 | Validation of CHARM multi-omics data against published datasets. **a**, Aggregated Hi-C contact maps for a 10-Mb region on chromosome 2 generated by CHARM, compared to aggregated single-cell data from Nagano et al. and bulk Hi-C data from Bonev et al. [1]. **b**, Pearson correlation matrix quantifying the similarity among contact maps in **a**. **c**, Pileup plot and heatmap showing enrichment of CHARM accessibility signals at ENCODE DNaseI peaks. **d**, Pileup plot and heatmap showing enrichment of CHARM H3K27me3 signals at ENCODE H3K27me3 peaks. **e-h**, Density scatter plots comparing CHARM data (x-axis) with public datasets (y-axis) for: **e**, A/B compartment scores (E1 eigenvector); **f**, RNA expression; **g**, chromatin accessibility; and **h**, H3K27me3 signal. Pearson's correlation coefficients are indicated.

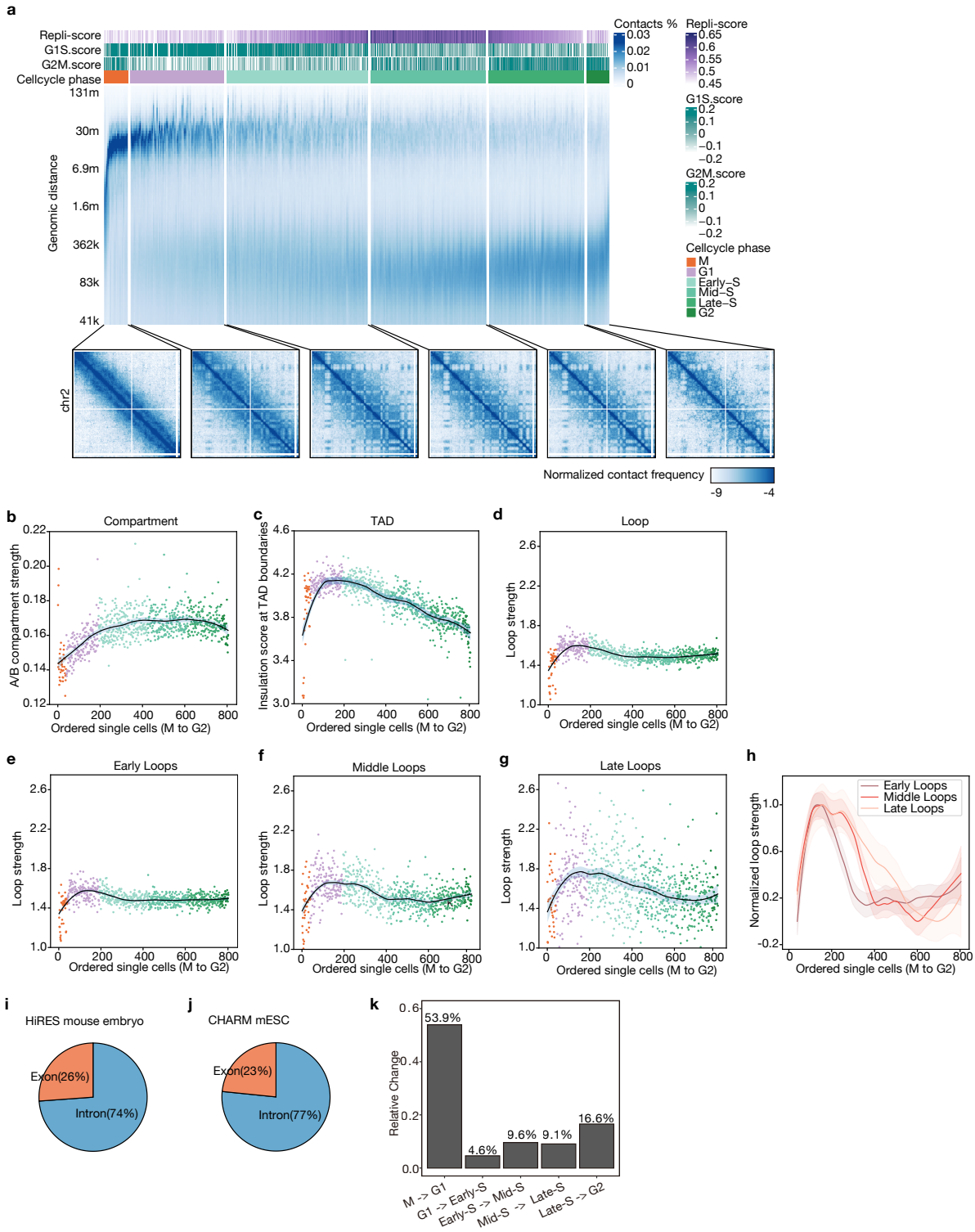

Supplementary Fig. 2 | Single-cell cell-cycle phasing using CHARM data. a, Single-cell contact decay profiles grouped by inferred cell-cycle phases with features used for annotating shown on top. Each row represents a genomic bin, and each column represents a single cell. ICE-

normalized aggregate contact maps for each cell-cycle phase are shown below. **b-d**, Dynamics of A/B compartments (b), topologically associating domains (TADs) (c), and chromatin loops (d) across the cell cycle. **e-g**, Same analysis as in d, with chromatin loops grouped by replication timing. Curves represent LOESS fits with 95% confidence intervals; each dot corresponds to a single cell. **h**, Overlaid min-max normalized curves from e-g showing loop dynamics across replication timing groups. Curves represent LOESS fits and shaded area represents the 95% confidence band. **i**,**j**, Pie charts showing the proportion of exonic and intronic UMIs detected in HiRES (**i**) and CHARM (**j**) datasets. **k**, Bar plot quantifying the relative increase in RNA UMI counts between consecutive cell-cycle phases.

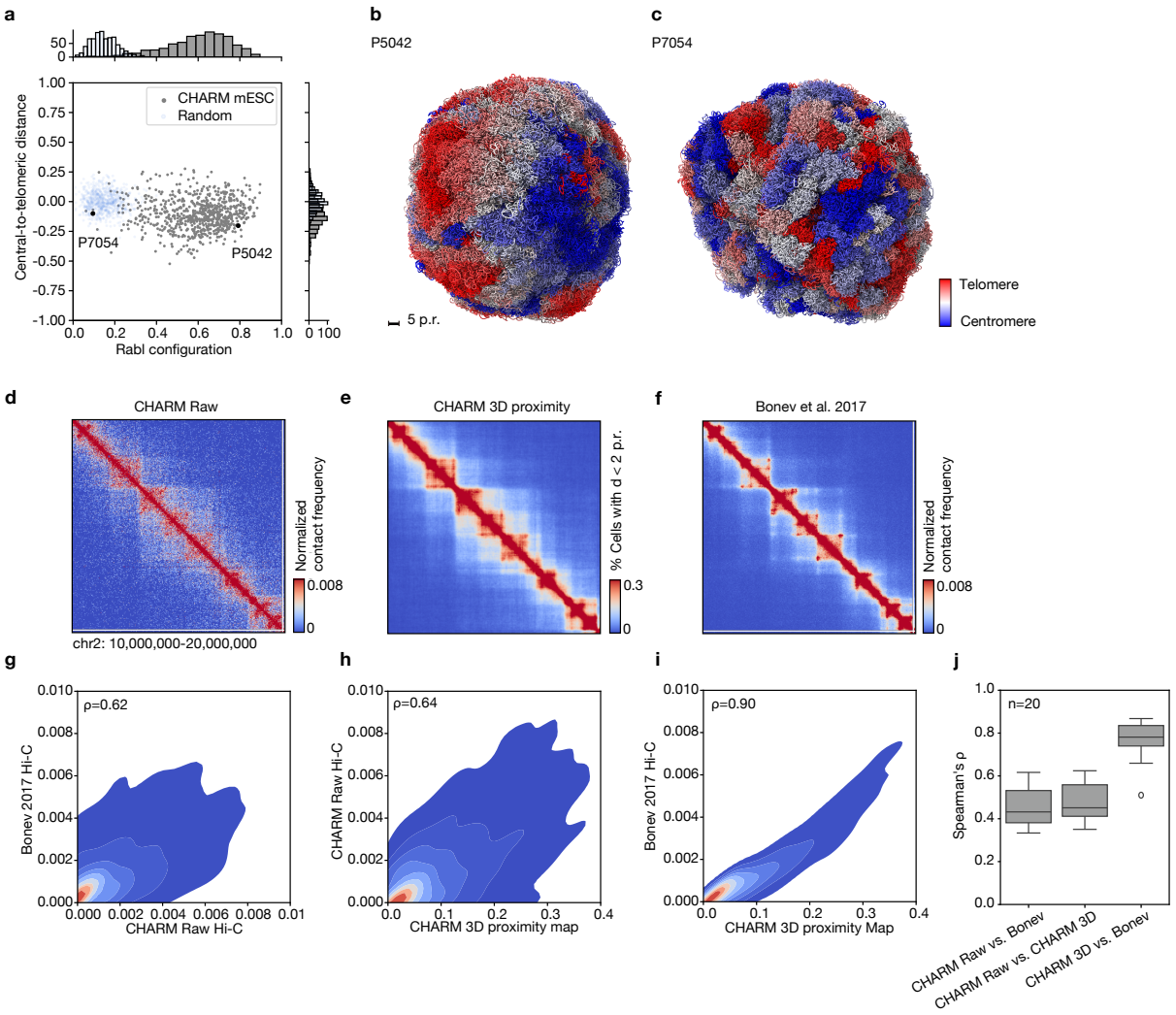

Supplementary Fig. 3 | Validation of 5-kb resolution single-cell 3D genome structures. a, Scatter plot quantifying the degree of Rabl configuration across all reconstructed single-cell structures. Random control values were obtained by, for each cell, generating the same number of centromere–telomere vectors with uniformly random orientations and computing the corresponding Rabl configuration score using the same procedure. **b,c**, Example 3D genome structures for two individual cells (P5042 and P7054) highlighted in **a**, colored by genomic position from centromere to telomere. **d-f**, Example maps for a representative 10-Mb region on chromosome 2, showing: **d,** CHARM single-cell aggregated Hi-C contact map; **e,** proximity map derived from CHARM-reconstructed 3D structures; and **f,** bulk Hi-C contact map from Bonev et al.[1] **g-i**, Density scatter plots comparing the contact maps in **d-f** pairwise, with Spearman's correlation coefficients (ρ) indicated. **j**, Box plots showing Spearman's correlation coefficients between CHARM contact maps, CHARM-derived proximity maps and bulk Hi-C contact maps across 20 randomly selected 10-Mb regions. Boxes indicate the median and 25th–75th percentiles, with whiskers extending to 1.5 times the interquartile range, points beyond the whisker represent outliers.

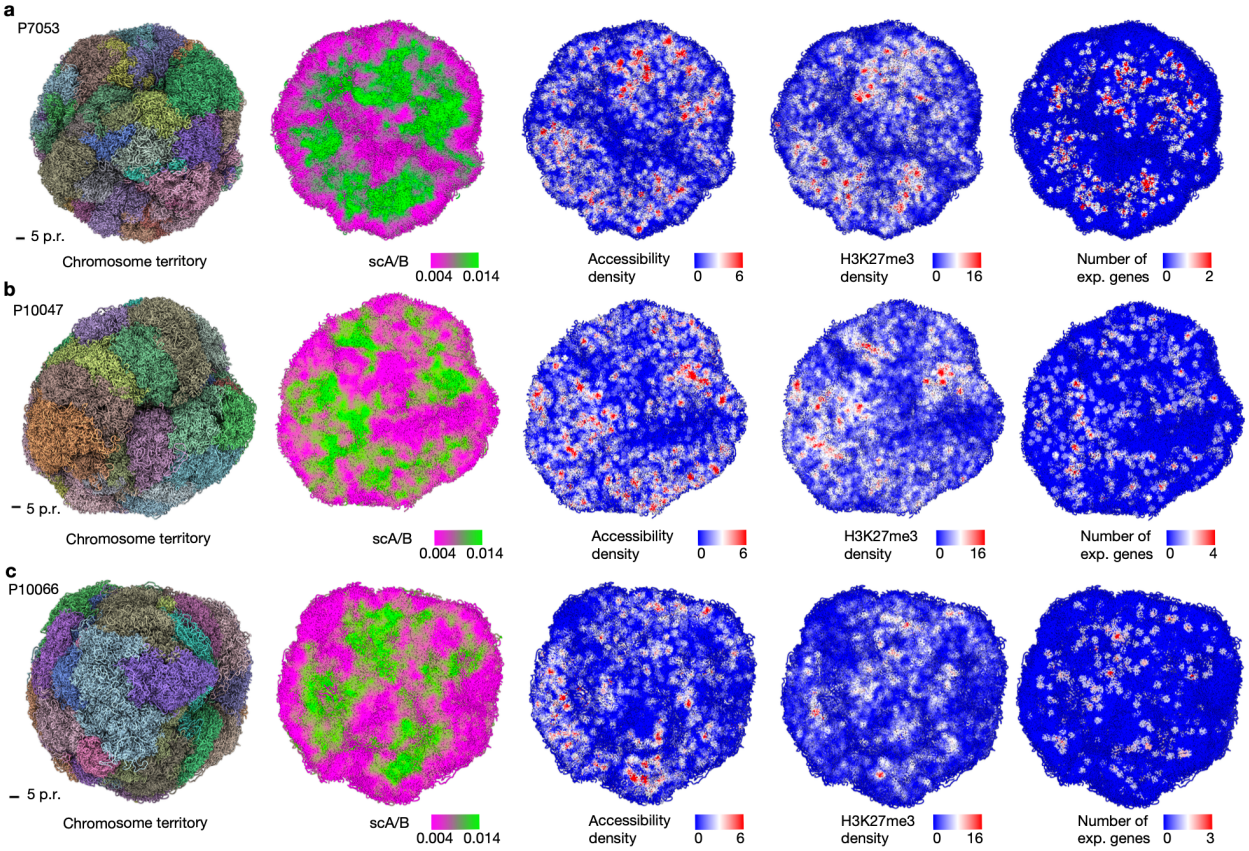

Supplementary Fig. 4 | Single cell 3D genome structures examples. Single cell 3D genome structures colored by associated data to illustrate the spatial distribution of multi-omics features; each panel shows a different cell (a-c).

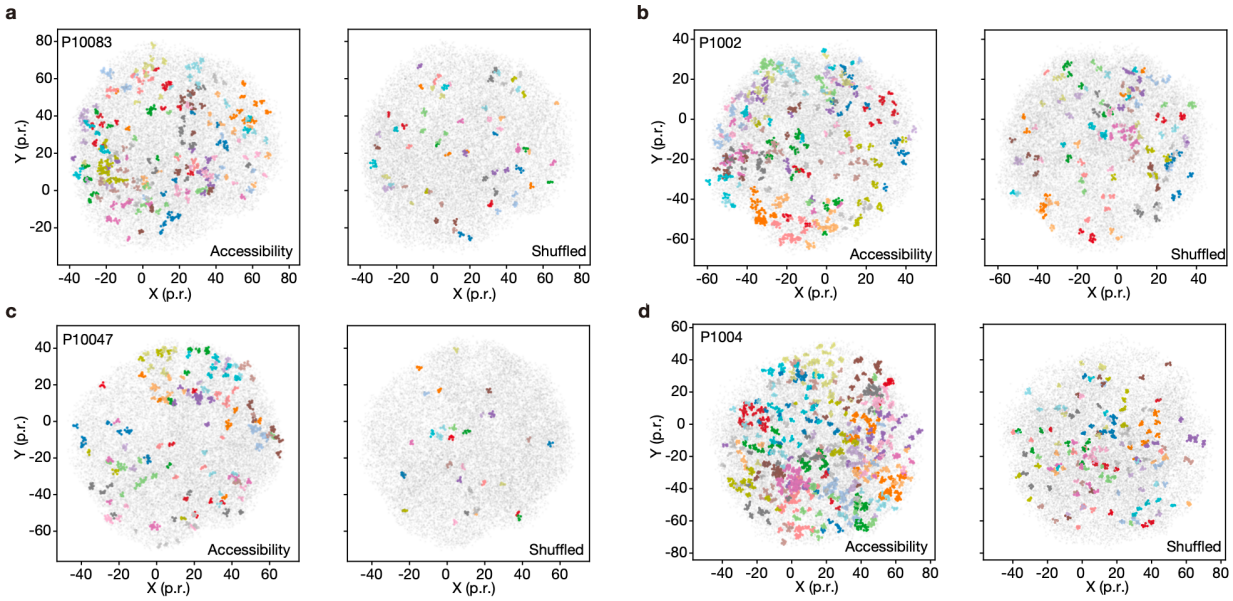

Supplementary Fig. 5 | Accessibility clusters examples. Z-projections of 3D accessibility clusters identified by DBSCAN (similar to Fig. 3g); each panel shows a different cell (a-d).

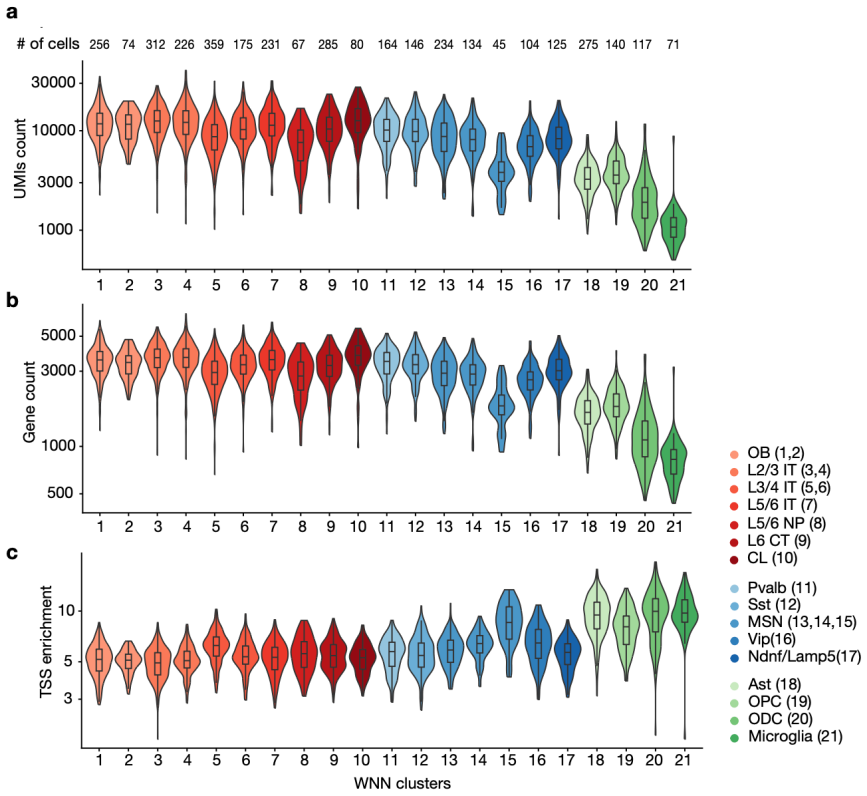

Supplementary Fig. 6 | Quality metrics across WNN clusters and annotated cell types. a-c, Violin plots showing per-cell total RNA UMI counts (a), number of detected genes (b), and TSS enrichment scores (c) across WNN clusters (x-axis; cluster IDs 1–21). Violins are colored by cell type annotations. Numbers above indicate the number of cells in each WNN cluster. Boxes indicate the median and 25th–75th percentiles, with whiskers extending to 1.5 times the interquartile range.

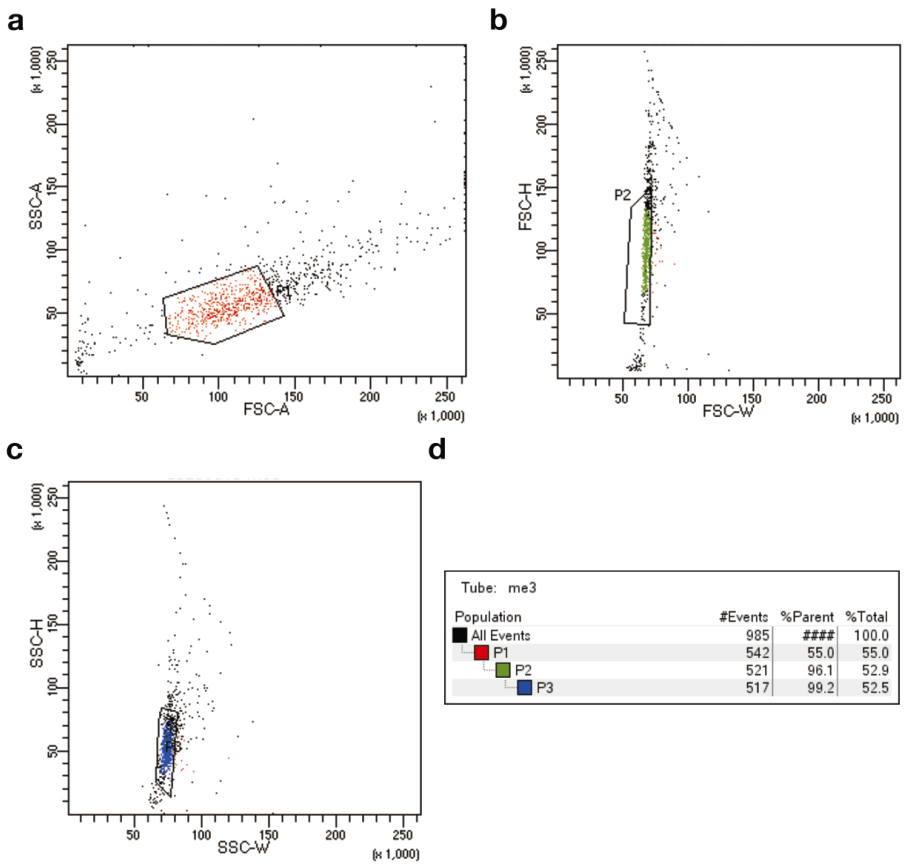

Supplementary Fig. 7 | Representative FACS gating strategy for nuclei singlet sorting. a–c, Sequential gates to remove debris (a), exclude doublets (b), and define singlets (c) for sorting. d, Representative event counts and percentages for each gated population.

Reference

1 Bonev, B. *et al.* Multiscale 3D Genome Rewiring during Mouse Neural Development. *Cell* **171**, 557-572 e524 (2017). https://doi.org/10.1016/j.cell.2017.09.043